UPPSALA
UNIVERSITET

Digital Comprehensive Summaries of Uppsala Dissertations from the Faculty of Science and Technology 749

A Theoretical Perspective on the Chemical Bonding and Structure of Transition Metal Carbides and Multilayers

MIKAEL RÅSANDER

ACTA
UNIVERSITATIS
UPSALIENSIS
UPPSALA
2010

ISSN 1651-6214
ISBN 978-91-554-7827-8
urn:nbn:se:uu:diva-123485

Dissertation presented at Uppsala University to be publicly examined in Häggsalen, Ångström Laboratory, Lägerhyddsvägen 1, Polacksbacken, Uppsala, Friday, June 11, 2010 at 10:15 for the degree of Doctor of Philosophy. The examination will be conducted in English.

Abstract
Råsander, M. 2010. A Theoretical Perspective on the Chemical Bonding and Structure of Transition Metal Carbides and Multilayers. Acta Universitatis Upsaliensis. *Digital Comprehensive Summaries of Uppsala Dissertations from the Faculty of Science and Technology* 749. 61 pp. Uppsala. ISBN 978-91-554-7827-8.

The present thesis deals with a theoretical description of issues regarding chemical bonding, structure and stability of transition metal carbides and multilayered structures.

First principles density functional theory has been used extensively to investigate the properties of alloyed solutions of transition metal carbides. Joint theoretical and experimental investigations have shown that there is a driving force for carbon to be released from these ternary carbide systems as a response to the alloying. This release of carbon was shown to yield favorable lubricating properties in the case of alloyed solutions of Ti-Al-C, that were not present in the case of pure TiC, a property that can be used to design new materials that combine high hardness with favorable tribological properties.

From calculations of the activation energy of C diffusion in the vicinity of substitutional transition metal impurities (M) in TiC, it is found that the mobility of C atoms is increased due to the presence of the impurities. The lowering of the activation energy barriers suggests that the mobility of C in alloyed solutions of Ti-M-C is increased and will be more pronounced at lower temperature than for C diffusion in TiC.

The magnetic properties of alloyed solutions of Ti-Fe-C has been investigated using both theory and experiment. Theoretical calculations reveal that the magnetic moment and the critical temperature increase when increasing the Fe content as well as when lowering the C content in the system. Furthermore, the magnetic exchange parameters between Fe atoms were found to clearly reflect changes in the chemical bonding when varying the C content. Experimentally the magnetic properties were found to be rather substantial. Furthermore, the magnetic properties changes upon annealing due to the formation of Fe-rich and Fe-poor regions in the system. After long enough annealing times precipitates of α-Fe are formed which is consistent with theoretical predictions.

The interaction between TiC(111) surfaces and C in the form of graphite has also been investigated. For these systems it was found that graphite was rather strongly bonded to the carbide surface and that the atomic as well as electronic structure at the interface depend on the termination of the carbide surface. This research was motivated by the recent interest in graphene, but also to investigate how carbide grains interacts with C when dispersed in a carbon matrix.

A model for the calculation of structural parameters in multilayer structures has been presented and evaluated. The model is based on classical elasticity theory and uses the elastic constants of the materials constituting the multilayer as the only input.

Keywords: Electronic structure, transition metal carbides, density functional theory, disorder, multilayers, chemical bonding, materials science

Mikael Råsander, Department of Physics and Astronomy, Materials Theory, Box 516, Uppsala University, SE-751 20 Uppsala, Sweden

© Mikael Råsander 2010

ISSN 1651-6214
ISBN 978-91-554-7827-8
urn:nbn:se:uu:diva-123485 (http://urn.kb.se/resolve?urn=urn:nbn:se:uu:diva-123485)

Till morfar.

List of Papers

This thesis is based on the following papers. In the thesis they are referred to by their Roman numerals.

I **Carbon release by selective alloying of transition metal carbides**
M. Råsander, E. Lewin, O. Wilhelmsson, B. Sanyal, M. Klintenberg, O. Eriksson, and U. Jansson, *submitted to Physical Review B* (2010).

II **A first principles study of the stability and mobility of defects in titanium carbide**
M. Råsander, B. Sanyal, U. Jansson and O. Eriksson, *in manuscript* (2010).

III **Surface and interface properties of graphene on titanium carbide - A first principles study**
M. Råsander, A. Bergman, A. Delin, B. Sanyal, U. Jansson, and O. Eriksson, *submitted to Physical Review B* (2010).

IV **Design of the Lattice Parameter of Embedded Nanoparticles**
E. Lewin, M. Råsander, M. Klintenberg, O. Eriksson and U. Jansson, *in manuscript* (2010).

V **Design of carbide-based nanocomposite thin films by selective alloying**
U. Jansson, E. Lewin, M. Råsander, O. Eriksson, B. André and U. Wiklund, *submitted to Surface & Coatings Technology* (2010).

VI **Wear-resistant magnetic thin film material based on $\mathbf{Ti}_{1-x}\mathbf{Fe}_x\mathbf{C}_{1-y}$ nanocomposite**
S. Bijelovic, M. Råsander, O. Wilhelmsson, E. Lewin, B. Sanyal, U. Jansson, O. Eriksson and P. Svedlindh, *Physical Review B*, **81**, 014405 (2010).

VII **Design of Nanocomposite Low-Friction Coatings**
O. Wilhelmsson, M. Råsander, M. Carlsson, E. Lewin, B. Sanyal, U. Wiklund, O. Eriksson, and U. Jansson, *Advanced Functional Materials*, **17**, 1611-1616 (2007).

VIII **Elasticity model for the evaluation of lattice parameters in multilayer systems**
M. Råsander, P. Souvatzis, A. Höglund and O. Eriksson, *in manuscript* (2010).

The following paper was co-authored by me but not included in this thesis.

1. **Pauli spin blockade in weakly coupled quantum dots**
   J. Fransson and M. Råsander, *Physical Review B*, **73**, 205333 (2006).

Reprints were made with permission from the publishers.

Contents

1. Introduction

We live in a world that is ruled by particles and their interactions. There are electrons, quarks, neutrinos and all other particles that together form the plethora of particles described by the standard model. For our everyday life however, the most important particles are the electrons. Together with the protons and neutrons, the electrons form the foundation of all elements of the Periodic Table. It is the electrons and their interactions that determine how molecules are formed from atoms and how atoms are combined to form solids. Within the field of materials physics the aim is to be able to understand the properties of various kinds of materials, from the atomic level to the condensed forms of the crystalline solids and the liquid state.

This thesis deals with a theoretical description based on first principles theory of issues regarding chemical bonding, structure and stability of materials that are of great interest, both from a scientific point of view and from an industrial perspective. To a great extent this thesis is concerned with the properties of transition metal carbides. For a long time these materials have been the focus of extensive research due to their many interesting physical properties and they are nowadays used in many technological applications. One example of such an application is as hard metal coatings on various components. Coatings are regularly used to protect surfaces in order to prolong different components life time. A bad or not well adapted coating material can severely shorten the life time, whereby a lot of attention has been given to investigations on how to design new coating materials with better functionality. As a part of this thesis an approach on how it is possible to design coating materials based on the transition metal carbides will be presented.

A traditional crystalline solid is an arrangement of atoms in some sort of lattice. This is in principle a homogeneous ordering with identical lattice positions where atoms occupy the different lattice sites. Nowadays, experimenters are able to manufacture superstructures in various forms. One example of such a structure is a multilayered material where different types of materials are grown on top of each other in a layered manner. These types of materials possess new properties and functionality, an example of which are the giant magneto resistance (GMR) effect for which Albert Fert and Peter Grünberg were awarded the Nobel Prize in Physics in 2007.

Theoretical investigations have always played a crucial role in the understanding of the physical world. The aim is here to obtain a description of all particles and how they interact by knowing only the number of particles and by

basing the description on fundamental laws of nature, i.e. from first principles or *ab initio*. For a solid or a liquid system it is very complicated to theoretically model and calculate different physical properties in such a way. This is due to the vast number of particles which constitute these many body systems. In order to obtain some useful information it is necessary to make a series of approximations and to setup elaborate models. In this work the density functional theory[1, 2] developed by Walter Kohn and co-workers has been used to calculate various materials properties. In essence the density functional theory converts the problem of many interacting particles and transforms it into a one particle problem which is much easier to solve. Various implementations of density functional theory are today among the most commonly used methods to perform calculations of the electronic structure of materials.

This thesis is divided into two parts. Part I is devoted to the theories of matter that have been used extensively in the research that is contained within this thesis. This part is not material specific and the discussion can be applied to any material of interest. In Part II there is a summary of the results presented in the attached papers which form the basis of this thesis, along with additional discussions concerning the properties of transition metal carbides and multilayered structures. Much of the work presented in this thesis has been performed in parallel with experimental investigations and this will be reflected when it comes to the discussion of the obtained results. However, the experimental techniques that have been used will not be described in any detail. For further details regarding the results the reader is directed to the original papers which are attached at the end of the thesis.

Part I:
Theory of the solid state

2. Introduction to the many body problem

In the solid state there are atoms which have condensed to form crystals out of free atoms. In free atoms the electrons move about the nucleus in atomic-like electron orbitals. In the condensed state these electrons begin to interact in between different atoms to form energy bands. The electronic structure in materials, which is the result of bringing atoms together, is what determines all materials properties. In this chapter we will discuss some of the theories and approximations that underlie the theoretical treatment of solid state systems.

The many body problem in condensed matter systems is of great importance, both when it comes to a complete understanding of the fundamental properties of these systems and to the understanding of materials for applications. Furthermore, it is one of the hardest problems to deal with, since the number of interacting particles is very large ($\sim 10^{23}$). To solve the problem as it is presented is analytically impossible and numerically intractable even when using top-of-the-line algorithms and computers. It is therefore imperative to make approximations in order to solve the problem at hand within a reasonable time.

The fundamental problem in condensed matter physics is the solution of the time-independent Schrödinger equation

$$\hat{H}\Psi = E\Psi, \tag{2.1}$$

where Ψ is the many particle wave function, E is the energy of the system, and $\hat{H}$ is the Hamiltonian given by

$$\hat{H} = -\frac{\hbar^2}{2M_N}\sum_{I=1}^{N_N}\nabla_I^2 - \frac{\hbar^2}{2m_e}\sum_{i=1}^{N_e}\nabla_i^2 + V(\{\mathbf{R}_I\},\{\mathbf{r}_i\}),^1 \tag{2.2}$$

where M_N is the mass of the nuclei, m_e the electron mass, N_N the number of nuclei, N_e the number of electrons, and $V(\{\mathbf{R}_I\},\{\mathbf{r}_i\})$ is the potential describing all interactions between electrons and nuclei, and $\hbar$ is Planck's constant. The potential is given by the sum of three different contributions:

$$V(\{\mathbf{R}_I\},\{\mathbf{r}_i\}) = V_{NN}(\{\mathbf{R}_I\}) + V_{ee}(\{\mathbf{r}_i\}) + V_{Ne}(\{\mathbf{R}_I\},\{\mathbf{r}_i\}), \tag{2.3}$$

[1] $\{\mathbf{R}_I\}$ and $\{\mathbf{r}_i\}$ are the positions of all nuclei and electrons respectively.

where

$$V_{NN}(\{\mathbf{R}_I\}) = \frac{e^2}{8\pi\varepsilon_o}\sum_{I\neq J}\frac{Z_I Z_J}{|\mathbf{R}_I - \mathbf{R}_J|} \tag{2.4}$$

is the interaction between different nuclei,[2]

$$V_{ee}(\{\mathbf{r}_i\}) = \frac{e^2}{8\pi\varepsilon_o}\sum_{i\neq j}\frac{1}{|\mathbf{r}_i - \mathbf{r}_j|} \tag{2.5}$$

is the electron-electron interaction, and

$$V_{Ne}(\{\mathbf{R}_I\},\{\mathbf{r}_i\}) = -\frac{e^2}{4\pi\varepsilon_o}\sum_{I,j}\frac{Z_I}{|\mathbf{R}_I - \mathbf{r}_j|} \tag{2.6}$$

is the electron-nuclei interaction.

To solve the problem presented in Eq. (2.1) for all particles in a solid is a very difficult task and one has to resort to approximations in order to manage it (the only problem that is solvable without approximations is in fact the hydrogen atom which can be solved analytically). In what follows a number of approximations will be given that are commonly used in the theory of the solid state.

2.1 The Born-Oppenheimer approximation

The Born-Oppenheimer or adiabatic approximation [3] is based on the fact that when considering the electronic structure, it is possible to neglect the kinetic energy of the nuclei in Eq. (2.2), since this term can be considered as small in relation to the other terms. This approximation relies on the fact that the mass of the nuclei is much larger than the mass of the electrons, $M_N >> m_e$. It may therefore be assumed, since the nuclei move so slowly compared to the electrons, that the electrons will move in an external potential from a static configuration of nuclei. It is therefore possible to formulate a Hamiltonian describing the electronic system as

$$\hat{H}_{el} = \hat{T} + \hat{V}_{ext} + \hat{V}_{int}, \tag{2.7}$$

where

$$\hat{T} = -\frac{\hbar^2}{2m_e}\sum_{i=1}^{N_e}\nabla_i^2 \tag{2.8}$$

[2] e is the elementary charge, Z_I is the atomic number, and ε_0 is the electric constant.

is the kinetic energy operator for the electrons,

$$\hat{V}_{ext} = V_{Ne} = \sum_{I,j} V_I(|\mathbf{R}_I - \mathbf{r}_j|) \tag{2.9}$$

is the external potential acting on the electrons due to the nuclei, and

$$\hat{V}_{int} = V_{ee} \tag{2.10}$$

is the internal potential describing the interaction between the electrons in the system. The electronic problem can now be solved via

$$\hat{H}_{el}\Psi_{el} = E_{el}\Psi_{el}.^{3} \tag{2.11}$$

The total energy of the system (electrons and nuclei), E_{tot}, can then be found as

$$E_{tot} = E_{el} + E_{II}, \tag{2.12}$$

where E_{II} is the energy contribution from a static configuration of nuclei that can be solved once and for all for a specific structure. We note that the interaction energy between the nuclei comes into the electronic problem as an additional constant energy shift. This shift does not change the form of the electronic wave function; the only contribution is a shift of the total energy of the system according to Eq. (2.12). The Born-Oppenheimer approximation effectively separates the electronic motion from the motion of the nuclei, and by doing so limits the complexity of the problem.

2.2 Bloch electrons

In a perfect crystal the ions are positioned in a periodic crystal lattice. The potential $V(\mathbf{r})$ then has the periodicity of the lattice

$$V(\mathbf{r}+\mathbf{R}) = V(\mathbf{r}), \tag{2.13}$$

for all translational lattice vectors $\mathbf{R}$. Assume for the moment that the electrons in the system are non-interacting and moving in a potential in the form of Eq. (2.13). Bloch's theorem then states that the wave function ψ of the one-electron Hamiltonian $H = -\hbar^2\nabla^2/2m + V(\mathbf{r})$ can be chosen to have the form of a plane wave times a function with the periodicity of the crystal [4]:

$$\psi_{n\mathbf{k}}(\mathbf{r}) = e^{i\mathbf{k}\cdot\mathbf{r}} u_{n\mathbf{k}}(\mathbf{r}), \tag{2.14}$$

where

$$u_{n\mathbf{k}}(\mathbf{r}+\mathbf{R}) = u_{n\mathbf{k}}(\mathbf{r}). \tag{2.15}$$

[3] In what follows, the subscripts in Eq. (2.11) will be neglected if there is no possibility of confusion.

The periodic functions $u_{n\mathbf{k}}(\mathbf{r})$ can be expanded using a basis set of plane waves whose wave vectors are reciprocal lattice vectors of the crystal:

$$u_{n\mathbf{k}}(\mathbf{r}) = \sum_{\mathbf{G}} c_{n\mathbf{k},\mathbf{G}} e^{i\mathbf{G}\cdot\mathbf{r}}, \tag{2.16}$$

where the $\mathbf{G}$'s are defined by $\mathbf{G}\cdot\mathbf{R} = 2\pi m$, where m is an integer. Each electronic wave function can then be written as a sum of plane waves:

$$\psi_{n\mathbf{k}}(\mathbf{r}) = \sum_{\mathbf{G}} c_{n,\mathbf{k}+\mathbf{G}} e^{i(\mathbf{k}+\mathbf{G})\cdot\mathbf{r}}. \tag{2.17}$$

The Bloch theorem with the periodicity of H and $V(\mathbf{r})$ greatly reduces the number of particles that have to be included in the evaluation of the wave function since it is now only necessary to solve the Schrödinger equation within the primitive unit cell.

2.3 Chemical bonding and forces between atoms

In solid state systems there are essentially four different types of chemical bonds: ionic, metallic, covalent and van der Waals (vdW) bonds, each with different characteristics. The ionic bond is characterized by an electron transfer from one atomic species to another, as in the case of salts, while the metallic bond is characterized by a more or less homogeneous distribution of electrons in space. The covalent bond in turn is characterized as the sharing of electrons between atoms. Most materials display a bonding character that is a mixture of all these different bonding types, to a varying degree. The bonding of the transition metal carbides as an example, which will be further discussed in Part II, shows a combination of covalent, ionic and metallic bonding, which is the reason for their interesting physical properties. The vdW bond, on the other hand, is much weaker than the other three types and in many system it is completely negligible, however, there are some famous cases where it is extremely important. One example of such a system is graphite where the vdW bond is solely responsible for the interlayer bonding between the graphite planes.

In order to find the most stable atomic configuration for a specific combination of atoms, it is necessary to calculate how much energy that can be gained by forming the crystal or molecule from individual atoms. This energy is the cohesive energy or the energy of formation. The stable ground state situation is found for the arrangement of atoms that gives the lowest energy of formation.

From a knowledge of the energy of a system for a specific atomic configuration it is possible to calculate the forces acting between all of the atoms by using the Hellmann-Feynman theorem [5, 6]. This theorem states that the

force acting on a nucleus is given by

$$\mathbf{F}_I = -\frac{\partial E}{\partial \mathbf{R}_I} = -\langle \Psi | \frac{\partial \hat{H}}{\partial \mathbf{R}_I} | \Psi \rangle = -\int n(\mathbf{r}) \frac{\partial \hat{V}_{ext}}{\partial \mathbf{R}_I} d\mathbf{r} - \frac{\partial E_{II}}{\partial \mathbf{R}_I}, \tag{2.18}$$

since the only terms in the Hamiltonian Eq. (2.7) that depend on the nuclei positions are the external potential $\hat{V}_{ext}$ and the nuclei-nuclei energy E_{II}. In Eq. (2.18) $n(\mathbf{r})$ is the unperturbed electron density given by

$$n(\mathbf{r}) = N \frac{\int d\mathbf{r}_2 \cdots d\mathbf{r}_N |\Psi(\mathbf{r}, \mathbf{r}_2 \cdots \mathbf{r}_N)|^2}{\int d\mathbf{r}_1 d\mathbf{r}_2 \cdots d\mathbf{r}_N |\Psi(\mathbf{r}_1, \mathbf{r}_2 \cdots \mathbf{r}_N)|^2}, \tag{2.19}$$

where N is the number of electrons and $\Psi(\mathbf{r}_1, \mathbf{r}_2 \cdots \mathbf{r}_N)$ is the N electron wave function given by Eq. (2.11). The expression for the force given in Eq. (2.18) makes it possible to perform dynamical simulations of condensed matter systems. For example, it is possible to perform molecular dynamics simulations [7, 8, 9], relax atoms into their local energy minimum [10], and to calculate phonon spectra [11, 12, 13]. Furthermore, the Hellmann-Feynman theorem gives another route towards finding the ground state structure of an atomic arrangement, since for the ground state the forces between atoms should be zero, i.e.

$$F_I = 0. \tag{2.20}$$

Also, it is possible to show from Eq. (2.18) that for a stable bonding situation to occur in a molecule or in a solid, there has to be electron charge being accumulated in-between the different atomic sites since the bare nuclei-nuclei interaction will otherwise be dominating and it would not be any minimum in the energy of the system. This is easiest to imagine for a diatomic molecule and as an example, consider the bonding situation in the hydrogen molecule, where the bonding state has a constructive interference between the two hydrogen wave functions in-between the two atoms, while the anti-bonding state has a destructive interference in this region. In this case the only possibility to have a stable situation is to occupy the bonding state [6, 14].

2.4 Order and disorder

Generally, in the condensed state there are two different types of disordered systems. There are the topologically or structurally disordered systems, where the atomic positions do not corresponding to any kind of underlying lattice. This is the situation in liquids and in amorphous solids. The other type of disorder is the substitutional disorder, which is when different atomic species occupy the positions on a crystalline lattice in a random uncorrelated fashion. This is the form of disorder that is present in random alloys. Disorder is hard to treat theoretically because many of the theories and approximations that

are valid in the crystalline solid, such as the Bloch theorem, breaks down in these states of matter. Materials where topological disorder is present reveal many interesting physical properties, however, such a discussion is beyond the scope of this section. Therefore, disorder will only be considered on a crystalline lattice. Good references for the discussion that will take place here are for example the book by Ducastelle [15] and the review article by Ruban and Abrikosov [16].

For a random alloy the different atoms are occupying the atomic positions of a crystal lattice. It is possible to define a correlation function for each position, $\xi_f^{(n)-pq\cdots s}$, according to

$$\xi_f^{(n)-pq\cdots s} = \langle c_i^{(p)} c_j^{(q)} \cdots c_k^{(s)} \rangle_f - c_p c_q \cdots c_s, \tag{2.21}$$

where $\langle \cdots \rangle_f$ denotes the ensamble average over all crystallographically equivalent n-site clusters of type f and c_p is the concentration of alloy component p. The $c_i^{(p)}$ are the occupation numbers, defined for each site i in the lattice, of the alloy component p. If the site i is occupied by species p the occupation number is identically equal to one, otherwise it is zero. When summed over all atomic sites the occupation number will give the concentration of the alloy component p. In a random alloy, the occupation of any cluster is uncorrelated and therefore $\xi_f^{(n)-pq\cdots s} = 0$.[4] The most important correlation function is the pair-correlation function. These can be re-written in a different form given by so called short range order (SRO) parameters

$$\alpha_m^{pq} = -\frac{\xi_m^{(2)-pq}}{c_p c_q}, \tag{2.22}$$

with $p \neq q$ and m is the coordination shell number. In the case of a binary alloy, $A_{1-x}B_x$, there is one SRO parameter for each shell. Then the maximum value for the SRO parameter is when $\alpha_m = 1$, which occurs when alloy component A only has A atoms at the shell m. This means that the atoms will form clusters. The other limit is when $\alpha_m = -x/(1-x)$, which means that perfect ordering occurs between the two components. For a completely random alloy the SRO parameters are identically zero. By means of the above defined correlation functions it is possible to set up elaborate ways of calculating properties of random alloys, for example it is possible to calculate the total energy of an alloy by using effective cluster interactions (ECI) [16].

The simplest method of treating disorder in a random alloy is the virtual crystal approximation (VCA). In the VCA, the potential at each atomic site is taken to be the average of the potential of the alloy components, so for a binary alloy with composition $A_{1-x}B_x$ the potential at each site will be given

[4] It should be noted that the definition of the correlation functions is not unique.

by

$$V^{\mathrm{A}_{1-x}\mathrm{B}_x} = (1-x)V^{\mathrm{A}} + xV^{\mathrm{B}}, \tag{2.23}$$

where $V^{\mathrm{A(B)}}$ is the potential for element A(B). The VCA is in many cases a much too crude approximation and it is therefore necessary to resort to more elaborate approximations.

The coherent potential approximation (CPA) is an upgraded version of the VCA, but instead of averaging the potential at each atomic site, within the CPA the average is performed over the scattering properties of the different atomic species when they are embedded in an effective medium. The scattering at each atomic site in the effective medium is taken to be equal to the average of the scattering properties of the alloy components in the effective medium. The scattering properties are then solved self-consistently to give the electronic properties of the alloy. The CPA is a much better method than the VCA, and it is a very successful method for treating disorder in random alloys [16]. However, local environment effects are difficult to treat appropriately in the CPA. Effects related to charge transfer can be treated by going beyond the single site approximation [17], however, local relaxations are problematic, why it is necessary for many systems to use other methods.

Another method of treating disorder in a random alloy is to use the supercell approach, where the different atomic species randomly occupy the different lattice sites. This method do take local environment effects, such as local relaxations, into account. However, when using such an approach while simply letting the different species randomly occupy the different sites, it is necessary to take averages over different supercells. This can easily become very cumbersome, especially if one considers large supercells. There is, however, another way of using the supercell approach, introduced by Zunger, which makes it possible to perform calculations of a random alloy with a certain composition by using only one configuration and that is by using so-called special quasi-random structure (SQS) [18, 19]. These structures are constructed in such a way that the correlation functions (described above) in the supercell are the best possible match to the correlation functions of the random alloy. A SQS will in this way mimic the disorder of the random alloy. The supercell methods have their advantage over the VCA or the CPA when considering local effects, such as local relaxation, due to the local distribution of atoms. However, these methods always introduce spurious periodic image interactions, since the supercell methods always use periodic boundary conditions and it would be necessary to have infinitely large supercells in order to remove periodic image effects completely. Still, the supercell methods are very efficient since interactions between atoms are the strongest at short distances and therefore, it is only required to use supercells that are large enough to capture the most important interactions in a proper fashion.

3. Density Functional Theory

When a quantum mechanical system is in the state $|\Psi\rangle$, the total energy of the system is given by the expectation value of the Hamiltonian, $\hat{H}$:

$$E[\Psi] = \frac{\langle\Psi|\hat{H}|\Psi\rangle}{\langle\Psi|\Psi\rangle}, \tag{3.1}$$

where

$$\langle\Psi|\hat{H}|\Psi\rangle = \int \Psi^* \hat{H} \Psi \, d\mathbf{r} \tag{3.2}$$

and

$$\langle\Psi|\Psi\rangle = \int \Psi^* \Psi \, d\mathbf{r}. \tag{3.3}$$

Since any measurement will give one of the eigenvalues of $\hat{H}$, we know that

$$E[\Psi] \geq E_0, \tag{3.4}$$

with E_0 being the ground state energy of the system. The ground state wave function is therefore given by the function that minimizes the energy, i.e.

$$E_0 = \min_{\Psi} E[\Psi]. \tag{3.5}$$

The ground state energy and ground state wave function are therefore determined by the minimization of the energy functional $E[\Psi]$, where the energy is written as a functional of the wave function, Ψ. Furthermore, the wave function that minimizes the total energy is the true ground state wave function.

In this chapter the density functional theory, developed by Walter Kohn and co-workers [1, 2] will be briefly described. The density functional theory do not express the energy of the system as a functional of the wave function, instead the energy is expressed as a functional of the particle density. For the discussion about to follow in this chapter there are excellent reviews, such as the books by Parr and Yang [20], Martin [21], and by Dreizler and Gross [22], as well as the review article by Jones and Gunnarsson [23], upon which the following discussion is based.

3.1 The Hohenberg-Kohn theorems

For a system described by the Hamiltonian in Eq. (2.7) with a determined number of electrons, N, the internal potential V_{int} is fixed while the external potential V_{ext} is determined by the number of nuclei. By setting the number of electrons and the external potential then completely determines all electronic properties. Hohenberg and Kohn [1] have shown that within a trivial additive constant, the external potential is determined by the ground state electron density $n(\mathbf{r})$. From this follows that the Hamiltonian is determined, except for a constant, and in turn the many body wave function. All properties of the system are therefore determined given the electron density alone. This is what usually is referred to as the first Hohenberg-Kohn theorem.

The second Hohenberg-Kohn theorem states that it is possible to define a universal functional $E[n]$ in terms of the density $n(\mathbf{r})$, for any external potential, such that the global minimum of $E[n]$ is the exact ground state energy of the system, and the density which minimizes $E[n]$ is the exact ground state density. Furthermore, the functional $E[n]$ alone is sufficient to determine the exact ground state energy and density.[1]

According to the first Hohenberg-Kohn theorem, all properties of the system are determined from the density and may therefore be considered as functionals of the density. The Hohenberg-Kohn functional, $E[n]$, can therefore be written as

$$\begin{aligned} E[n] &= T[n] + E_{int}[n] + \int V_{ext}(\mathbf{r}) n(\mathbf{r})\, d\mathbf{r} \\ &\equiv F[n] + \int V_{ext}(\mathbf{r}) n(\mathbf{r})\, d\mathbf{r}, \end{aligned} \tag{3.6}$$

where $F[n] = T[n] + E_{int}[n]$ contains the contribution to the energy functional from the internal electronic degrees of freedom.

The Hohenberg-Kohn theorems are exact, and density functional theory described so far is therefore an exact theory. However, the Hohenberg-Kohn theorems are merely theorems of existence in-as-much that they do not prescribe a recipe for finding the energy functional. So far no one has found an exact functional and in order to continue it is necessary to come up with schemes on how to proceed.

3.2 The Kohn-Sham method

The Kohn-Sham method [2] is to replace the difficult problem of many interacting electrons obeying the Hamiltonian in Eq. (2.7) with an auxiliary system that can be solved more easily. The auxiliary system may be chosen in a variety of ways, however, Kohn and Sham assumed that the ground state density of the original system of interacting electrons is equal to that of a specific non-interacting system. This leads to independent particle equations for the

non-interacting system that can be solved exactly, where all difficult many body terms have been incorporated into an exchange-correlation functional of the density.

The Kohn-Sham method begins with rewriting the Hohenberg-Kohn energy functional in Eq. (3.6) in the form

$$E_{KS} = T_s[n] + \int V_{ext}(\mathbf{r}) n(\mathbf{r})\, d\mathbf{r} + E_H[n] + E_{xc}[n], \tag{3.7}$$

where

$$T_s[n] = -\frac{\hbar^2}{2m_e} \sum_{i=1}^{N} \langle \phi_i | \nabla^2 | \phi_i \rangle, \tag{3.8}$$

is now the independent electron kinetic energy and

$$E_H[n] = \frac{e^2}{8\pi\varepsilon_0} \int \frac{n(\mathbf{r}) n(\mathbf{r}')}{|\mathbf{r} - \mathbf{r}'|}\, d\mathbf{r} d\mathbf{r}' \tag{3.9}$$

is the Hartree energy. The term $E_{xc}[n]$ is the exchange-correlation energy. Since the goal is to calculate the total energy of the system, Eqs. (3.6) and (3.7) are required to be equal, and by comparison

$$E_{xc}[n] = F[n] - (T_s[n] + E_H[n])\,. \tag{3.10}$$

By varying the Kohn-Sham energy functional Eq. (3.7) with respect to the density $n(\mathbf{r})$ one finds the Kohn-Sham equation

$$\left[-\frac{\hbar^2}{2m_e} \nabla^2 + V_{ext}(\mathbf{r}) + V_H(\mathbf{r}) + V_{xc}(\mathbf{r}) \right] \phi_i(\mathbf{r}) = \varepsilon_i \phi_i(\mathbf{r}), \tag{3.11}$$

with

$$V_H(\mathbf{r}) = \frac{e^2}{4\pi\varepsilon_0} \int \frac{n(\mathbf{r}')}{|\mathbf{r} - \mathbf{r}'|}\, d\mathbf{r}' \tag{3.12}$$

being the Hartree potential and

$$V_{xc}(\mathbf{r}) = \frac{\delta E_{xc}[n(\mathbf{r})]}{\delta n(\mathbf{r})} \tag{3.13}$$

being the exchange-correlation potential. The three potentials in Eq. (3.11) may be grouped together in an effective potential $V_{eff}[n]$.

The electron density is given by sum of squares of the Kohn-Sham orbitals

$$n(\mathbf{r}) = \sum_{\sigma} \sum_{i=1}^{N} |\phi_i(\mathbf{r})|^2, \tag{3.14}$$

where we have introduced the summation over spins, $\sigma = \uparrow, \downarrow$. It is now possible by solving the Kohn-Sham equation (3.11) from a given effective potential to find the Kohn-Sham eigenvalues ε_i and the Kohn-Sham orbitals ϕ_i and from these calculate the density of a system of N non-interacting electrons. Furthermore, by remembering that the potential of a system is a functional of the density, it is possible to solve the Kohn-Sham equation, Eq. (3.11), self-consistently, by starting from an initial density $n_{in}(\mathbf{r})$.

The total energy may be found by noticing that all terms in the Kohn-Sham energy functional E_{KS} given by Eq. (3.7) are explicitly dependent on the density except for the kinetic energy T_s given by Eq. (3.8), which is only implicitly depending on the density via the orbitals ϕ_i. However, by solving the eigenvalue problem given by Eq. (3.11) for the eigenvalues ε_i the kinetic energy may be expressed in the form

$$T_s = E_s - \int V_{eff}(\mathbf{r}) n(\mathbf{r})\, d\mathbf{r}, \tag{3.15}$$

with

$$E_s = \sum_{\sigma=\uparrow,\downarrow} \sum_{i=1}^{N} \varepsilon_i^{\sigma}. \tag{3.16}$$

The kinetic energy can now be readily calculated along with the other terms in Eq. (3.7). The total energy of the system can therefore be calculated iteratively, by starting from an initial density, finding the corresponding potentials, solving the Kohn-Sham equation, and then evaluating a new density. If the new density is close enough to the original density the total energy is evaluated, otherwise, some mixture of the old and new densities are used as a new input, and this process is continued until self-consistency is acquired.

3.3 Approximations for the exchange-correlation energy functional

The Kohn-Sham method outlined in the previous section has its advantage that almost everything in the Kohn-Sham energy functional, Eq. (3.7), can be calculated exactly. The problem is the exchange-correlation functional, since the form of this functional is not known and it is therefore necessary to resort to approximations of this term. There are nowadays many approximations for this functional [21, 24]. The simplest approximation is the local density approximation (LDA) [2, 25, 26], in which it is assumed that the exchange-correlation energy is an integral over all space with an exchange-correlation energy density at each point equal to the corresponding energy density of a

homogeneous electron gas with the same density, i.e.

$$E_{xc}[n^{\uparrow}, n^{\downarrow}] = \int n(\mathbf{r}) \varepsilon_{xc}^{hom}(n^{\uparrow}(\mathbf{r}), n^{\downarrow}(\mathbf{r}))\, d\mathbf{r}, \tag{3.17}$$

where $\varepsilon_{xc}^{hom}(n^{\uparrow}(\mathbf{r}), n^{\downarrow}(\mathbf{r}))$ is the exchange-correlation energy per particle in a homogeneous electron gas with density $n^{\sigma}(\mathbf{r})$. The LDA works very well for being such a simple approximation. The reason for this is that many solids may be considered close to the limit of the homogeneous electron gas. When the electron density no longer may be considered to be homogeneous the LDA is expected to be less useful and it is necessary to use more advanced functionals.

In the so called generalized-gradient approximations (GGAs) the LDA is taken a step further and functionals are introduced that not only depend on the density at a point but also the magnitude of the gradient of the density at a point $|\nabla n^{\sigma}|$. The exchange-correlation energy functional can in this case be written as

$$E_{xc}^{GGA}[n^{\uparrow}, n^{\downarrow}] = \int n(\mathbf{r}) \varepsilon_{xc}(n^{\uparrow}(\mathbf{r}), n^{\downarrow}(\mathbf{r}), |\nabla n^{\uparrow}(\mathbf{r})|, |\nabla n^{\downarrow}(\mathbf{r})|)\, d\mathbf{r}. \tag{3.18}$$

There are many varieties of the GGA, among the most commonly used in actual calculations are the ones created by Becke (B88) [27], Perdew and Wang (PW91) [28], and by Perdew, Burke and Enzerhof (PBE) [29]. For many properties the GGA is an improvement over the LDA, bonds in molecules are more accurately described by the GGA than with the LDA for example.

There are also other improvements to the exchange-correlation functional that can be made [21] to improve on the accuracy of the Kohn-Sham method, however in the calculations performed in this thesis only the LDA and the GGA approaches have been used.

4. Plane waves, pseudopotentials and PAW's

The Kohn-Sham equation, Eq. (3.11), presented in the previous chapter is a Schrödinger-like equation, describing a single electron moving in an effective potential:

$$\left[-\frac{\hbar^2}{2m_e}\nabla^2 + V_{eff}(\mathbf{r})\right]\phi_i(\mathbf{r}) = \varepsilon_i\phi_i(\mathbf{r}). \tag{4.1}$$

In solid state physics there are mainly two different approaches towards solving the above equation; Hamiltonian methods that rely on a direct diagonalization of the Hamiltonian and Green's function based methods. The Hamiltonian methods utilize an expansion of the orbitals ϕ_i into some kind of basis functions according to

$$\phi_i = \sum_k c_k^{(i)}\xi_k, \tag{4.2}$$

where ξ_k is some type of basis function and the $c_k^{(i)}$ are expansion coefficients. The expansion can be performed in many different ways, for example it is possible to use plane waves as a basis in all of space, or one can use augmented methods where space is divided into regions and different kinds of functions are used as basis in the various regions. The difference in the way the expansion is performed has given rise to many different methods that are used regularly in electronic structure calculations, such as plane wave pseudopotential methods, augmented plane wave methods, as well as the muffin-tin based methods. The Green's function based methods on the other hand rely on single-particle Green's functions which describe the propagation of electrons from different points in space. The different methods have their advantages and disadvantages. In this chapter the focus is on the way Eq. (4.1) is solved when the expansion in Eq. (4.2) is in terms of plane waves.

If the system of interest is a crystal it is known from the Bloch theorem discussed in Chapter 2 that the wave functions may be described by a plane wave multiplied by a function with the periodicity of the lattice. Plane waves of the form $e^{i\mathbf{q}\cdot\mathbf{r}}$ may be used to effectively describe the periodic function and the Kohn-Sham orbitals may then be expanded in the form

$$\phi_{n\mathbf{k}}(\mathbf{r}) = \sum_{\mathbf{G}} c_{n,\mathbf{k}+\mathbf{G}} e^{i(\mathbf{k}+\mathbf{G})\cdot\mathbf{r}}, \tag{4.3}$$

where $\mathbf{G}$ is a reciprocal lattice vector and the $c_{n,\mathbf{k}}$'s are plane wave coefficients that remain to be determined. The Kohn-Sham equation expressed in terms of a plane wave basis then has the form

$$\sum_{\mathbf{G}'} \left[\frac{\hbar}{2m_e} |\mathbf{k}+\mathbf{G}|^2 \delta_{\mathbf{G}\mathbf{G}'} + V_{eff}(\mathbf{G}-\mathbf{G}') \right] c_{n,\mathbf{k}+\mathbf{G}'} = \varepsilon_n c_{n,\mathbf{k}+\mathbf{G}}. \tag{4.4}$$

In principle, an infinite number of plane waves need to be involved in the solution of the above equation. However, the plane wave coefficients $c_{n,\mathbf{k}+\mathbf{G}}$ with small kinetic energy, $(\hbar^2/2m_e)|\mathbf{k}+\mathbf{G}|^2$, are more important than those with high kinetic energy. It is therefore possible to expand the wave functions in a finite basis by only considering those plane waves with a kinetic energy below a specified cut-off energy. This cut-off introduces an error in the calculation, but this error can be controlled by checking the convergence of the total energy with respect to increased basis size [10].

The expansion of the wave function in terms of plane waves has a number of advantages, e.g. a plane wave expansion is a conceptually easy basis set, it is relatively easy to implement in a computer code, fast Fourier transforms between real and reciprocal space may be used and the kinetic energy operator has a nice diagonal form. However, there is a serious problem when trying to describe the wave functions in the core region of atoms, since the wave functions in this region is rapidly varying. It is therefore necessary to include a large number of plane waves in the basis to accurately describe the wave function in this region.

4.1 Pseudopotentials

A fact of nature is that most physical properties of solids, bonding for example, depend on the valence electrons to a much greater extent than on the electrons in the core. The pseudopotential approximation makes use of this fact by replacing the strong ionic potential by a weaker pseudopotential that acts on pseudo wave functions instead of on the true wave functions. The concept behind the pseudopotential is illustrated in Fig. 4.1. The valence wave functions oscillate rapidly in the region close to the core. These oscillations occur since the valence wave functions must be orthogonal to the core wave functions, because of the exclusion principle. The pseudo wave functions are then constructed in such a way that they have identical scattering properties off the ions and core electrons as the valence wave functions, but also so that they have no radial nodes in the core region [21, 10], see Fig. 4.1.

Pseudopotentials have been used for a long time in electronic structure calculations. In order to have a good pseudopotential it is necessary for the potential to be transferable, so that the same potential may be applied to different problems. Norm-conserving pseudopotentials are examples of potentials that

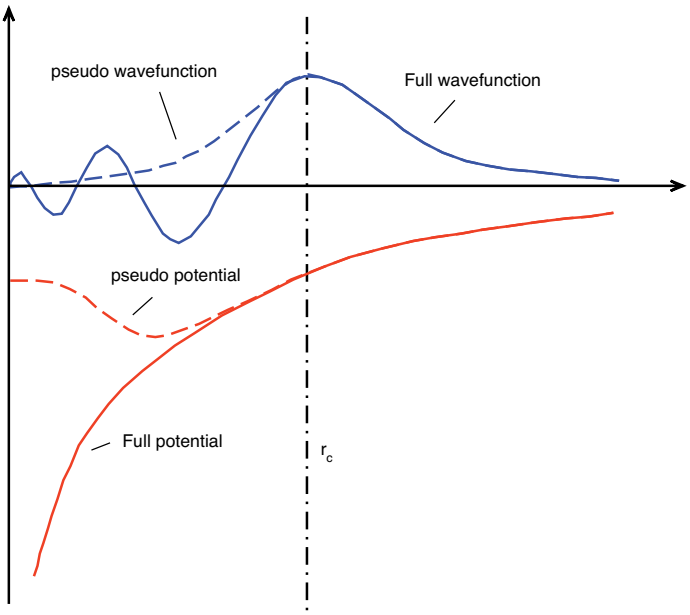

Figure 4.1: Illustration of the concept behind the pseudopotential. The pseudo wave function coincides with the true or full valence wave function at the cut-off radius r_c and beyond. Similarly, for the pseudopotential.

not only have the property that the all-electron and pseudo wave function coincide beyond the cut-off radius but also that the integrated charge inside r_c is identical. These norm-conserving potentials are both accurate and transferable.

One aim when constructing pseudopotentials is to make the potential as smooth as possible, meaning that the potential is constructed so that the plane wave basis set that has to be used is as small as possible. The norm-conserving potentials are accurate but the size of the basis set is still required to be large leading to large computational costs. By using so-called ultrasoft (US) pseudopotentials [30, 31] it is possible to perform accurate calculations while having a smooth potential. The concept behind this approach is to divide the problem into two parts; one smooth function and another auxiliary function around each ion core that represents the rapidly varying part of the density. In the next section another method will described that can be adapted into the pseudopotential concept which increases the accuracy beyond both the norm-conserving and US pseudopotantials, namely the projector augmented wave method.

4.2 Projector augmented waves

The projector augmented wave (PAW) method, due to Blöchl [32], is another general method to solve the electronic structure problem. By combining the properties of the augmented plane wave (APW) method and the pseudopotential method it is possible to have access to the full wave functions, which is impossible in the pseudopotential method, while maintaining a limited size of the basis set.

The strategy of APW methods is to divide the wave functions into two parts: a partial wave expansion within an atom centered sphere and envelope functions outside the spheres. The envelope functions are then expanded into plane waves or some other basis set. Partial wave expansion and envelope functions are then matched at the sphere radius. The PAW method, however, utilizes a transformation of the valence wave functions onto fictitious pseudo wave functions according to

$$|\phi\rangle = \mathscr{T}|\tilde{\phi}\rangle, \tag{4.5}$$

where $|\phi\rangle$ is the true all-electron (AE) valence wave function and $|\tilde{\phi}\rangle$ the pseudo (PS) wave function. By knowing the transformation from the PS wave functions to the AE wave functions, it is possible to evaluate expectation values $\langle\hat{A}\rangle$ for an operator $\hat{A}$ in terms of the PS wave functions instead of the AE wave functions. Especially, it is possible to evaluate the total energy as a function of the PS wave functions and end up with a Kohn-Sham equation for the PS wave functions according to

$$\mathscr{T}^{\dagger}\hat{H}\mathscr{T}|\tilde{\phi}\rangle = \varepsilon\mathscr{T}^{\dagger}\mathscr{T}|\tilde{\phi}\rangle. \tag{4.6}$$

The transformation $\mathscr{T}$ is defined to differ from identity only by a sum of local atom-centered contributions:

$$\mathscr{T} = \mathbf{1} + \sum_{\mathbf{R}} \hat{\mathscr{T}}_{\mathbf{R}}, \tag{4.7}$$

where each local contribution $\hat{\mathscr{T}}_{\mathbf{R}}$ acts only within an augmentation region $\Omega_{\mathbf{R}}$ enclosing the atom at $\mathbf{R}$. This implies that the PS and AE wave functions coincide outside the augmentation region. The local operators $\hat{\mathscr{T}}_{\mathbf{R}}$ are defined for each augmentation region by specifying a set of target functions $|\phi_i\rangle$ for the transformation $\mathscr{T}$ for a set of initial functions $|\tilde{\phi}_i\rangle$ that are orthogonal to the core states and complete within the augmentation region. We call these functions, following Blöchl's terminology [32], AE and PS partial waves respectively. The relation between them is

$$|\phi_i\rangle = (\mathbf{1} + \hat{\mathscr{T}}_{\mathbf{R}})|\tilde{\phi}_i\rangle \tag{4.8}$$

within $\Omega_{\mathbf{R}}$. The next step is to express the PS wave function as

$$|\tilde{\phi}\rangle = \sum_i |\tilde{\phi}_i\rangle c_i \tag{4.9}$$

within $\Omega_{\mathbf{R}}$. So the PS wave function inside the augmentation region is a sum of PS partial waves multiplying constants c_i. The corresponding AE wave functions can also be expressed, within $\Omega_{\mathbf{R}}$, as

$$|\phi\rangle = \mathscr{T}|\tilde{\phi}\rangle = \sum_i |\phi_i\rangle c_i. \tag{4.10}$$

The coefficients c_i are scalar products and can be written as

$$c_i = \langle \tilde{p}_i | \tilde{\phi} \rangle, \tag{4.11}$$

with $\langle \tilde{p}_i|$ being projector functions, one for each partial wave and fulfilling the condition $\sum_i |\tilde{\phi}_i\rangle\langle \tilde{p}_i| = 1$ within $\Omega_{\mathbf{R}}$. This implies that the expansion $\sum_i |\tilde{\phi}_i\rangle\langle \tilde{p}_i|\tilde{\phi}\rangle$ is identical to $|\tilde{\phi}\rangle$ itself and in turn that $\langle \tilde{p}_i|\tilde{\phi}_j\rangle = \delta_{ij}$ within the same augmentation region. The linear transformation $\mathscr{T}$ may therefore be written as

$$\mathscr{T} = \mathbf{1} + \sum_i \left(|\phi_i\rangle - |\tilde{\phi}_i\rangle \right) \langle \tilde{p}_i|, \tag{4.12}$$

and accordingly the AE wave functions is expressed as

$$|\phi\rangle = |\tilde{\phi}\rangle + \sum_i \left(|\phi_i\rangle - |\tilde{\phi}_i\rangle \right) \langle \tilde{p}_i|\tilde{\phi}\rangle. \tag{4.13}$$

Any operator $\hat{A}$ can now be transformed to act on the smooth PS wave functions according to

$$\tilde{A} = \mathscr{T}^{\dagger}\hat{A}\mathscr{T} = \hat{A} + \sum_{i,j} |\tilde{p}_i\rangle \left(\langle \phi_i|\hat{A}|\phi_j\rangle - \langle \tilde{\phi}_i|\hat{A}|\tilde{\phi}_j\rangle \right) \langle \tilde{p}_i|. \tag{4.14}$$

By using Eq. (4.14) it is possible to write the the total density at a point $\mathbf{r}$ as

$$n(\mathbf{r}) = \tilde{n}(\mathbf{r}) + n_1(\mathbf{r}) + \tilde{n}_1(\mathbf{r}), \tag{4.15}$$

where the first term is a smooth part arising from the density of PS wave functions, while the last two terms are one-center terms that depend on the AE and PS partial waves respectively, within each augmentation region. A similar decomposition can also be done for the total energy. By effectively separating the problem into different parts, the PAW method allows for an efficient treatment of separated problems, while at the same time it offers the possibility for implementation of the PAW method in plane wave pseudopotential codes. By using plane waves for a basis the PAW method has become a very useful method, with the ability of performing accurate calculations with a limited basis set size [33].

Part II:
Transition metal carbides and multilayers

5. Transition metal carbides

The transition metal carbides (TMC) are materials that have attracted large interest, due to their combination of many interesting physical properties. This combination of physical properties has given these materials many different forms of industrial applications, for example as hard metal coatings on various machine components. In this chapter some general properties of TMC will be presented along with a summary of the results presented in Papers I to VII.

5.1 General properties of transition metal carbides

The TMC that will be the focus of this chapter are known as interstitial carbides, meaning that the crystal structure is built up by a metallic lattice, where the carbon atoms occupy the interstitial positions of the lattice. Since there are many different types of crystal structures that metal atoms can form, there are naturally many different forms of carbide structures. In Figure 5.1 there are illustrations of TMC in the B1 (or NaCl) and B_h (or WC) structures. These

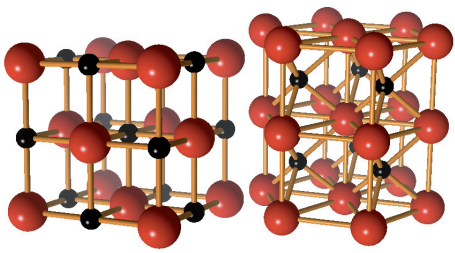

Figure 5.1: Illustration of the crystal structure of metal carbides in the B1 (a) and B_h (b) structures. Metal atoms is represented by the red spheres and carbon atoms by black spheres.

materials are known for their many interesting physical properties, such as high hardness and high melting temperatures. In fact, some of the melting temperatures are among the highest ever measured [34]. The TMC also possess high electrical and thermal conductivities. A striking feature of these carbides is their defect structure. Ideal stoichiometry is almost never found and

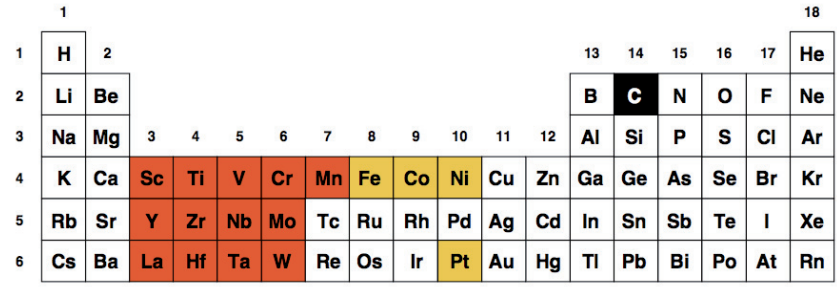

Figure 5.2: Illustration of the Periodic Table with the transition metal elements that are involved in carbide formation is highlighted. The elements with orange coloring are strong carbide formers, while the elements with yellow coloring form metastable carbides [38, 39, 40].

the carbide phases exist over a broad range of compositions, TiC_{1-y} for example is stable for carbon vacancy concentrations, y, ranging from about 0.05 to 0.45. The reason for the combination of different properties is closely related to the chemical bonding in the carbides, which display a combination of covalent, metallic and ionic flavors to a varying degree [34, 35, 36, 37]. The most prominent bonding in these systems is however, the covalent bonds that are formed between metal d- and carbon p-electrons.

Carbide formation is quite common among the transition metal elements, which is illustrated in Fig. 5.2. The early transition metals in group 3 to 6 of the Periodic Table are strong carbide formers and form thermodynamically stable carbides with various crystal structure and stoichiometry. The late transition metals in group 8 to 10 form metastable carbides and are therefore known to be weak carbide formers [34, 38, 39, 40].

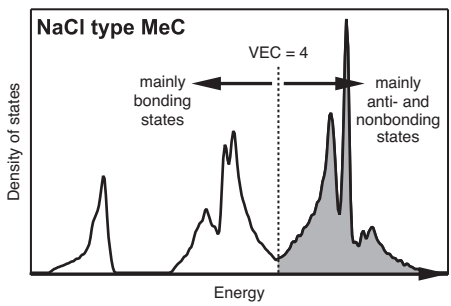

Figure 5.3: Illustration of the density of states of TMC in the B1 or NaCl crystal structure. The Fermi level of TiC is given by the vertical dotted line. The valence electron concentration (VEC) is here given per atom.

Since the structure of TMC consist of binary lattices, the formation of a carbide involves an expansion of the metal lattice in order to make room for the carbon atoms. Fortunately, when the carbon atoms are in place bonds between metal and carbon atoms are created that make up for the loss in energy due to the expansion of the metal lattice [41, 42, 43, 44, 45]. By restricting the discussion to TMC in the B1 or rock salt crystal structure, the stability of the TMC varies throughout the transition metal (TM) series. The most stable carbides are found for TM in group 4; Ti, Zr and Hf. The reason for this is illustrated in Fig. 5.3 for the case of the 3d TM. Generally, the electronic structure of these carbides display a rigid band behavior when varying the TM in the carbide. The density of states (DOS) shown in Fig. 5.3 has been calculated for TiC. With 4 valence electrons per atom contributing to the bonding, the Fermi level of TiC is positioned in a valley in the DOS that separates bonding states from anti- and non-bonding states [42, 45, 46]. The TMC in this group are therefore maximally bonded and by increasing or decreasing the number of electrons the carbide will become less stable due to the occupation of anti-bonding states or because of the lower occupation of bonding states. Another interesting fact concerning the bonding in the TMC is that carbides in the rock salt structure become dynamically unstable if the valence electron concentration is larger than 9, whereupon a phase transition should occur [47, 48]. In what follows, the fact that the TM have a varying tendency for carbide formation will be used to see how the stability changes when stable monocarbides are alloyed with elements that have a weak carbide forming ability.

5.2 Alloying of carbides and carbon release

As mentioned in the previous section, the TMC are known to be chemically stable compounds. However, the ability to form stable carbides varies throughout the Periodic Table. While some elements are good carbide formers, such as Ti and W, other elements such as Ni, Cu or Al do not form any stable forms of carbides, at least not when considering the traditional carbide compounds. In Figure 5.4 the calculated formation energy of $Ti_{1-x}M_xC$ in the rock salt structure is shown, where M is any of the 3d transition metal atoms. The energy of formation has been calculated according to

$$E_{Form} = E(\mathrm{Ti}_{1-x}\mathrm{M}_x\mathrm{C}) - (1-x)\cdot E(\mathrm{Ti}) - x\cdot E(\mathrm{M}) - E(\mathrm{C}).^{1} \qquad (5.1)$$

It is clear that the formation energy increases as a function of the alloying. A negative formation energy signifies a stable ternary solution while a positive value in this case means that the alloyed carbides will decompose into more stable phases. Also shown in Fig. 5.4 is the calculated energy for carbon to be

[1] Here and throughout the remaining parts of the thesis $E(\mathrm{X})$ means the total energy of the compound or element X.

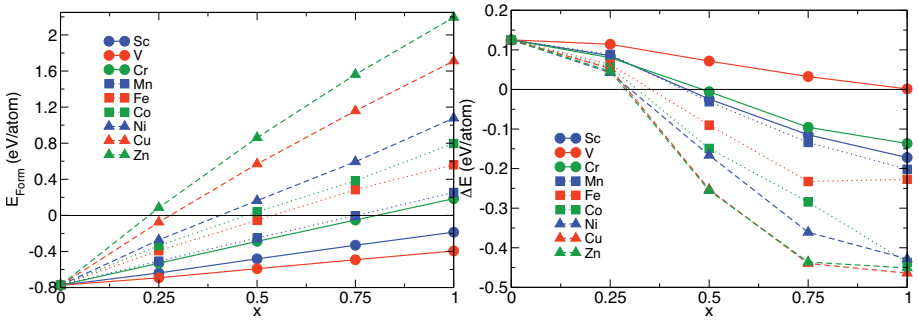

Figure 5.4: The calculated formation energy of alloyed $Ti_{1-x}M_xC$ for alloying TiC with other metals from the 3d transition metal series as a function of the alloying component x (a) and the calculated energy difference for carbon segregation defined by Eq. (5.2) (b). From Paper I.

released from the carbide, calculated according to

$$\Delta E = E(Ti_{1-x}M_xC_{1-y}) + y \cdot E(C) - E(Ti_{1-x}M_xC), \tag{5.2}$$

where the reference state for carbon is graphite. Negative values mean that carbon will be released from the carbide and it is clear that carbon release correlates with the increased formation energy of $Ti_{1-x}M_xC$.

In Figure 5.5 experimental results obtained by X-ray diffraction (XRD) and X-ray photoelectron spectroscopy (XPS) is given for the case of TiC alloyed with Ni. The XRD results show that Ni is dissolved in the carbide on the Ti lattice and that no segregation of Ni is apparent. Furthermore, results from the XPS show that as a response of the alloying there is an increased amount of C-C bonds in the alloyed samples, suggesting that carbon has been released. This is visible for both as deposited samples and as a response to annealing. For further discussions on this see Paper I.

The results presented here and in Paper I show that there is a driving force for the release of carbon from alloyed $Ti_{1-x}M_xC$, the strength of which depends on the composition and which element has been used as the alloying component. This release of carbon may be utilized to obtain new functionality of the TMC. This was investigated in Paper VII. Here the alloying component was Al and it was found from both theoretical calculations and from experimental measurements that carbon was released from the carbide. It was also shown that the friction coefficient of these systems is lowered in the alloyed samples than when compared to samples which contained no Al. These materials may therefore be used as hard and durable coating materials, which also possess an inherent drive for self-lubrication upon external pressures and

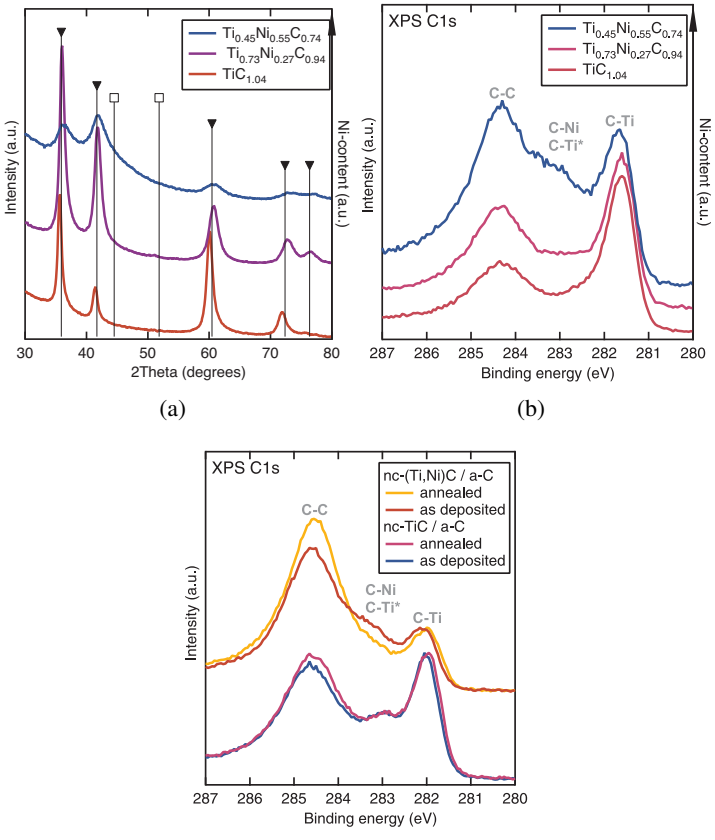

Figure 5.5: X-ray diffraction data (a), and X-ray photoelectron spectra of as-deposited (b) and annealed (c) samples of $Ti_{1-x}Ni_xC_{1-y}$. From Paper I.

elevated temperatures. A general review of the experimental and theoretical situation of ternary thin films of TMC is given in Paper V.

5.3 Stability and mobility of defects

The ability for TMC to release carbon is not solely depending on the driving force for carbon release. The carbon atoms must also be mobile, which means that it must be possible for them to move. In Figure 5.6 the activation energy barriers for C vacancy mediated diffusion and for a C atom to move from a octahedral to a tetrahedral site is given for a supercell of TiC. These barriers have been calculated using the nudged elastic band technique [49, 50, 51, 52], which is ideal for calculations of energy barriers since the method maps out

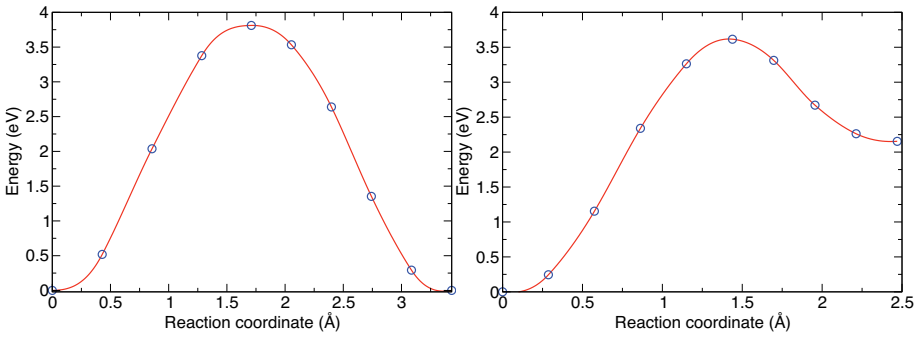

(a) (b)

Figure 5.6: Calculated activation energy barrier for carbon vacancy mediated diffusion (a) and the energy required to move a C atom from an octahedral to a tetrahedral position (b) in TiC.

the minimum energy path between an initial and a final geometry. The barriers in Fig. 5.6 are in good agreement with experimental findings [38]. However, the experimental situation is complex due to the varying stoichiometry of TiC. What can be concluded is however, that the energy required for C diffusion to be activated is high, which means that the carbides must be heated to high temperatures in order for carbon to diffuse in the crystal. It is therefore interesting to see how the carbon diffusion processes changes when a smaller or larger amount of foreign elements are introduced in a binary carbide, especially when regarding carbon release from alloyed TMC which was discussed in the previous section.

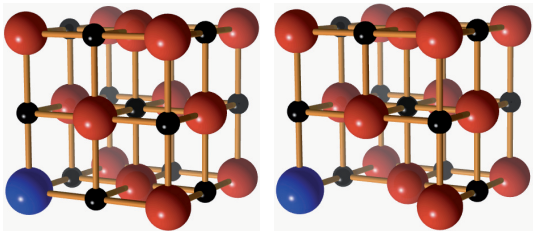

(a) (b)

Figure 5.7: TiC in the B1 crystal structure with the defects considered in Paper II. Figure (a) shows the case of a single substitutional 3d TM impurity (blue) while Figure (b) depicts the situation when a C vacancy is present at the nearest neighbor C position to the TM impurity. Ti and C are illustrated by the red and black spheres respectively.

Table 5.1: *Calculated defect formation energies obtained using Eqs. (5.3) and (5.4) for single metal substitutions and carbon vacancies in TiC. Note that there is no substitutional defect in the case of Ti. The activation energy, E_A is given for C vacancy driven diffusion. Also shown are the lattice parameters of the binary 3d TM carbides in the B1 structure, a_{B1}.*

Element	a_{B1} (Å)	E_s (eV)	E_v (eV)	E_A (eV)
Sc	4.68	1.08	0.33	4.71
Ti	4.34	n.a.	0.61	3.81
V	4.15	0.74	0.46	3.01
Cr	4.07	2.25	0.04	2.47
Fe	3.99	3.76	-0.38	2.05
Co	4.01	4.10	-0.40	2.20
Ni	4.08	4.65	-0.54	2.45
Cu	4.24	5.95	-0.71	2.68
Zn	4.40	7.08	-0.83	2.98

In Paper II we report on the stability of substitutional 3d transition metal (TM) defects and their effect on the local surrounding in TiC, especially when regarding bonding to carbon. Furthermore, activation energy barriers for C diffusion was investigated. The main results are summarized in Table 5.1, where the energy of formation of a single 3d TM substitutional impurity,

$$E_s = E(\mathrm{TiC;M}_s) - E(\mathrm{TiC}) - (E(\mathrm{M}) - E(\mathrm{Ti})), \tag{5.3}$$

as well as the formation energy of carbon vacancies, in the vicinity of TM defects,

$$E_v = E(\mathrm{TiC;C}_v) - E(\mathrm{TiC}) + E(\mathrm{C}), \tag{5.4}$$

are shown, together with calculated lattice parameters of the different TMC in the B1 structure. Activation energy barriers for vacancy driven carbon diffusion in TiC is also shown in Table 5.1. These barriers are for the case of C vacancy driven diffusion in the presence of the TM impurities, i.e. a C atom positioned at the nearest neighbor C position to a TM impurity moves to a vacant C position at another nearest neighbor position to the TM impurity. For further details see Paper II. The different defects considered are illustrated in Fig. 5.7. It is seen in Table 5.1 that the energy required to form the substitutional TM defects, E_s, increases the further to the right of the Periodic Table the defect element is positioned. This energy is also very high, suggesting a very low solubility of these TM in TiC, which implies that alloyed solutions of $\mathrm{Ti}_{1-x}\mathrm{M}_x\mathrm{C}$, discussed previously, are indeed metastable. Furthermore, the energy of formation of creating a C vacancy close to the TM impurity, E_v,

is lower in the vicinity of the impurity than in pure TiC, which means that the C atoms close to impurities are much more loosely bonded. In fact, as can be seen in Table 5.1, for Fe, Co, Ni, Cu and Zn the vacancy formation energy is negative which means that these vacancies will be formed spontaneously. These observations can be explained by different elements ability to form carbides. However, the activation energy barriers for vacancy mediated C diffusion do not decrease monotonously when changing the TM. The barriers are lower for the weak carbide formers than in pure TiC, however, the barrier in the presence of Sc is higher than in pure TiC and towards the end of the series there is an increase of the height of the barrier. This behavior follows the behavior of the lattice parameters of the 3d TMC in the B1 crystal structure which is also shown in Table 5.1. Therefore the behavior of the activation energy barriers is attributed to both a decreased ability for the TM to form carbides as well as to an atomic size effect due to the correlation with the lattice parameters in the 3d TMC. Based on these results it is possible to conclude that the introduction of impurities in TiC affects the distribution of C vacancies, since the vacancies tend to be closer to the impurities, and that it also has an effect on the mobility of C atoms in the carbide. These results suggest that the ability for alloyed solutions of carbides to release carbon will set in at lower or higher temperatures depending on the alloying element.

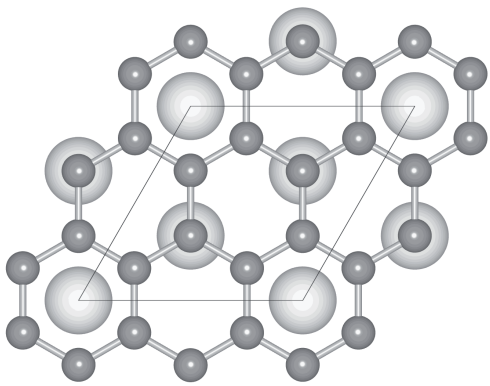

Figure 5.8: The $\sqrt{3} \times \sqrt{3}R30$ surface geometry of graphene/graphite on TiC(111) when the carbide surface is terminated by Ti. C atoms are represented by dark grey spheres and Ti atoms by light grey spheres.

5.4 Properties of carbide-carbon interfaces

It is already established that the carbides have many favorable properties and have therefore been used in many applications. One such application is as coating materials. A widely studied carbide coating material is nanocompos-

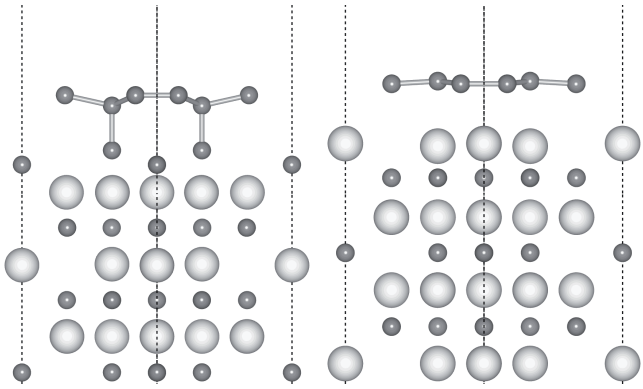

Figure 5.9: Relaxed surface structure of the TiC(111) surface and monolayer of graphite when (a) the carbide surface is C terminated and (b) when the surface is Ti terminated. C atoms are represented by dark grey spheres and Ti atoms by light grey spheres. For more details see Paper III.

ites of carbide grains dispersed in an amorphous carbon matrix, nc-MC/a-C, where M can be any TM. Since these materials contain grains of carbides in a C matrix the interaction between the interfaces is an important issue to understand. In Paper III the interface properties of the TiC(111) surface and layers of graphene/graphite were investigated. Graphene, a 2 dimensional allotrope of carbon has during recent years attracted great interest due to its special properties, which has spawned many investigations on how to make this material and how it interacts with other materials [53, 54]. The investigation in Paper III was therefore motivated by the recent interest in graphene and how it interacts with different surfaces and also to model the carbide grain and C matrix interface bonding in nc-TiC/a-C. The way graphene was placed on TiC(111) is shown in Fig. 5.8. Due to the crystal structure of TiC, the TiC(111) surface can be terminated in two different ways; either completely by C or completely by Ti. The termination of the carbide surface was found to influence the structural relaxations at the interface, which is shown in Fig. 5.9, as well as the chemical bonding between carbide and graphene. However, irrespective of the surface termination, the graphene layer directly on top of the surface was found to have a metallic density of states at the Fermi level. The same results were obtained in the model calculations on TiC grains in a C matrix, where layers of graphene were sandwiched in between layers of TiC(111) surfaces.

Furthermore, by using Bader analysis [55, 56, 57, 58] it was established that a transfer of electrons from the carbide to the C atoms on the Ti terminated surface occurs. This is shown in Fig. 5.10 where the difference in the charge

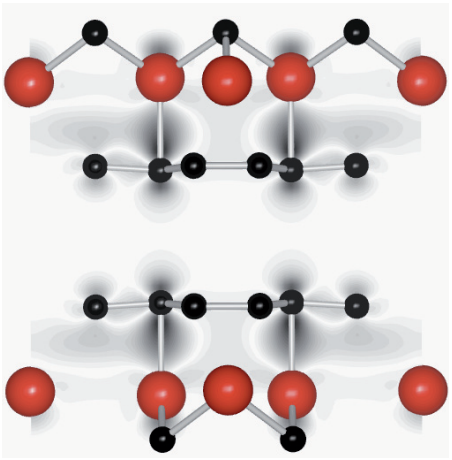

Figure 5.10: Calculated interface structure of bi-layers of graphite sandwiched between two TiC(111) surfaces. Here Ti atoms are illustrated by the red spheres while C atoms is illustrated by black spheres. Also shown is a charge density difference plot along a plane that cuts right through the interface model. For details see Papers III and IV.

density is plotted for a plane that cuts the interface model perpendicular to the (111) surface. As can be seen in Fig. 5.10, there is an accumulation of charge between C atoms in the graphene/graphite and the Ti atoms of the carbide surface that has a larger weight on the C side. This electron transfer from the carbide will lead to carbide grains depleted in electrons. In Paper IV, the effects of this charge depletion was investigated and found to yield an increase of the lattice parameter of the carbide. The increase in the lattice parameter of electron deficient TiC nicely correlates with an experimental observation, that the lattice parameter of TiC grains in an amorphous C matrix increases when the size of the grains becomes smaller.

5.5 Magnetic properties of $Ti_{1-x}Fe_xC_{1-y}$

In Paper VI, we investigated the magnetic properties of thin films of $Ti_{1-x}Fe_xC_{1-y}$ from both theory and experiment. Here the Kohn-Korringa-Rostoker (KKR) method [59, 60] in connection with the atomic sphere approximation (ASA) [61, 62] was used to solve the electronic structure problem. This is a Green's function based method which is perfectly adopted to be used together with the coherent potential approximation (CPA).

The magnetic moments, magnetic exchange parameters and electronic structure of completely random $Ti_{1-x}Fe_xC_{1-y}$ were calculated while varying the Fe content x and the C vacancy concentration y. By using the magnetic

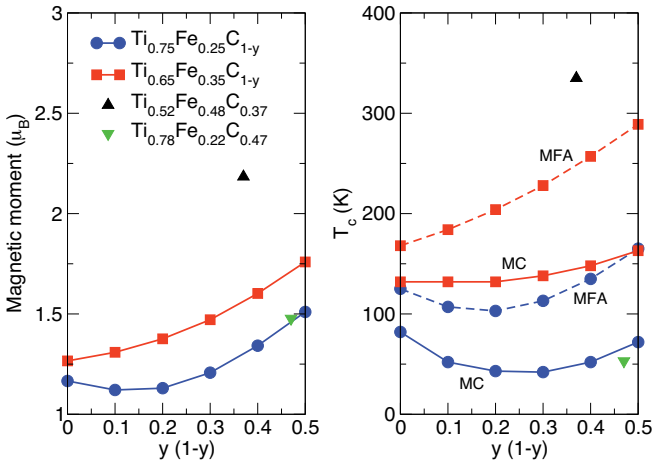

Figure 5.11: The calculated magnetic moment and transition temperatures for $Ti_{1-x}Fe_xC_{1-y}$ for $x = 0.25$ and 0.35 as a function of y. Also shown are the specific cases of $(x,y) = (0.48,0.63)$ and $(x,y) = (0.22,0.53)$. For these specific points the data is given as a function of $1-y$.

exchange parameters the critical temperatures of the system was obtained by means of both the mean field approximation (MFA) as well as by performing Monte Carlo simulations (MC). For more details see Paper VI. The results are given in Fig. 5.11. The general conclusion is that the magnetic properties (magnetic moments and critical temperature T_c) increase when increasing the amount of Fe and when lowering the C content. Furthermore, it was found that the exchange parameters clearly reflect the changes in the chemical bonding in the system when lowering the C content. The exchange parameters for $x = 0.35$ and different values for y are given in Fig. 5.12. Note that the behavior of the exchange parameters varies when changing the C content. For low C vacancy concentrations the nearest neighbor interaction is smaller than the second nearest neighbor interaction, while for large vacancy concentrations the nearest neighbor interaction is the largest. This behavior comes from the difference in the chemical bonding in these situations. The bonding in TiC is, which was discussed in Section 5.1, known to be primarily due to covalent bonds between Ti and C, however, when the number of vacancies on the carbon lattice increases the influence of the d-electron interaction between metal atoms will become more pronounced. It is this change in behavior that is reflected in Fig. 5.12.

The calculations of the magnetic properties of $Ti_{1-x}Fe_xC_{1-y}$ were all performed for a system where Fe as well as C vacancies were randomly dispersed on each of the sublattices. However, as was pointed out in Section 5.2, these ternary carbide phases are highly metastable and possess a driving force for phase separation into more stable phases. After annealing, $Ti_{1-x}Fe_xC_{1-y}$-

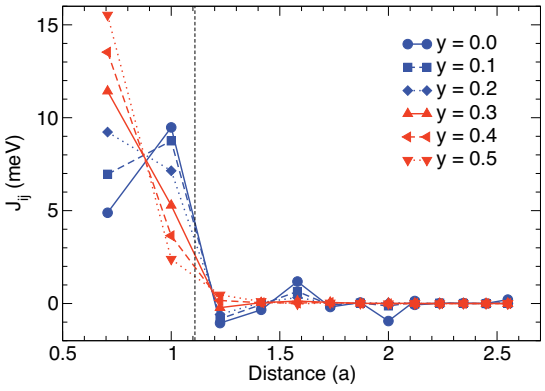

Figure 5.12: The calculated interatomic exchange parameters, J_{ij}, between Fe atoms in $Ti_{1-x}Fe_xC_{1-y}$ for $x = 0.35$ for different C vacancy concentrations, y, as a function of distance. Where the distance is given in terms of the lattice parameter of the crystal.

phases were found (see Paper VI) to phase separate into Fe-rich regions and TiC-rich regions as depicted in the tunnel electron microscopy (TEM) images in Fig. 5.13. The experimentally measured moments and critical temperatures were found to be rather substantial and to reflect the formation of Fe-rich phases upon annealing. The trend of phase separation into Fe-rich regions inside the carbide shown in Fig. 5.13 is an interesting avenue for the creation of magnetic tri- or multilayers that can be used as wear-resistant magnetic thin-film materials.

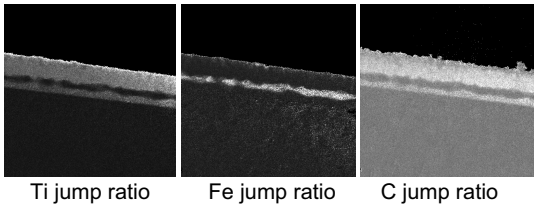

Figure 5.13: TEM images of a $Ti_{1-x}Fe_xC_{1-y}$ film deposited on MgO(100) showing Ti-, Fe- and C-rich regions (brighter contrast indicate higher element concentration), signifying a phase separation into a Fe-rich phase and TiC.

6. Structure of multilayered materials

By growing materials, layer by layer, in a controlled fashion has opened a venue for new properties and functionality. Often atoms can be grown epitaxially, i.e. on top of each other, so that the same crystal structure is maintained as the interface between different materials is traversed. One of the most studied examples of such materials are the multilayer structured materials, which is illustrated in Fig. 6.1. In these multilayer structures it has been observed that the physical properties are coupled to the structural arrangement of the atoms in the multilayers.

From a theoretical perspective, the detailed geometry of multilayer structures is a very complicated problem to treat in a realistic fashion, since the number of atoms involved in any calculations of this type is necessarily large. For this reason, it is necessary to use simple methods to predict the structure of multilayers.

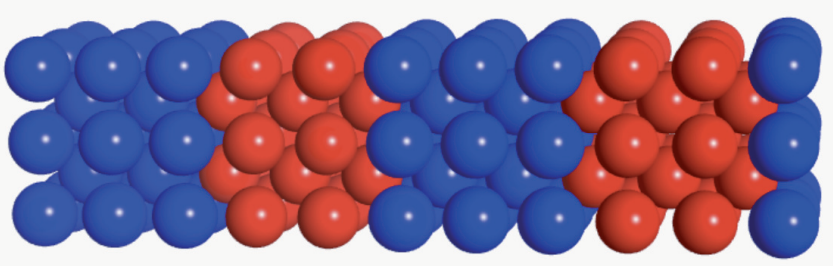

Figure 6.1: Illustration of a multilayered system where the multilayer components have the same thickness. Blue and red spheres represent different types of elements.

When performing first principles calculations on multilayers there are several approximations that are commonly used. One way is to assume that one subsystem in the multilayer completely dominates the other and that it is possible to use the same lattice parameter in the whole system. This approximation works the best when one of the sublayers is thin in comparison to the other. However, for multilayers with comparable thickness this approximation does not work as good. Another approximation is the use of Vegard's law, which is a phenomenological observation from alloyed systems, which states that the lattice parameter of an $A_{1-x}B_x$ alloy is a linear combination of the lattice parameters of the two subsystems, i.e. $a_{A_{1-x}B_x} = (1-x)\cdot a_A + x\cdot a_B$. This

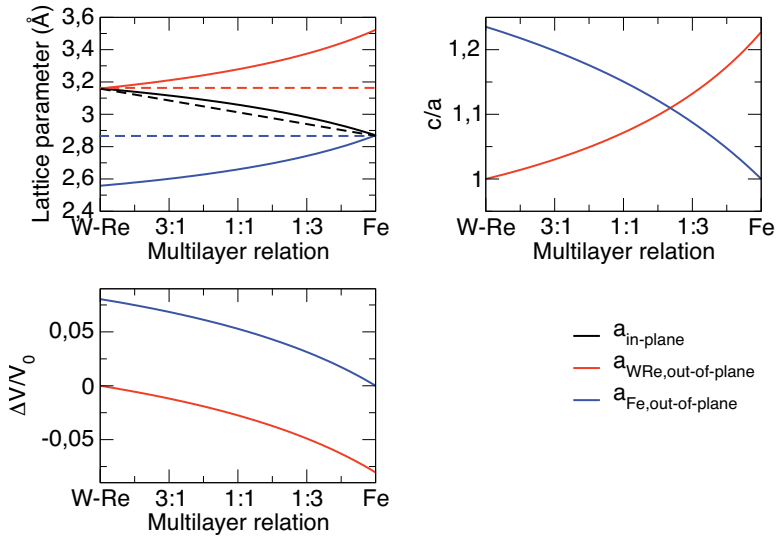

Figure 6.2: Calculated in- and out-of-plane lattice parameters of $W_{0.8}Re_{0.2}$/Fe multilayers, c/a-ratio and relative change in the volume in each sublayer as obtained by the elasticity model presented in Paper VIII. ΔV is the difference in volume of a component in the multilayer compared to the single crystal bulk value V_0. On the x axis the relation between $W_{0.8}Re_{0.2}$ and Fe is given.

approximation can give reliable results, however, the structure is still assumed to be the same throughout the multilayer, which may not be the case in the experimental situation.

In Paper VIII we have evaluated a model which is based on elasticity theory, which can in a more realistic fashion consider different structural relaxations within each subsystem of the multilayer. The model assumes perfect lattice matching at the interface between the different subsystems and that the elastic properties within each layer are the same in the multilayer as they are in the pure bulk crystals. This model gives more reliable structural parameters than the previously mentioned approximations and the structures generated by this model serves as a good starting point for the evaluation of physical properties of various kinds of multilayers. In Figure 6.2 results are shown for calculations using the elasticity model for multilayers consisting of Fe and a $W_{0.8}Re_{0.2}$ alloy grown along the [100] direction of the body centered cubic lattice. The in-plane lattice parameter, defined as the lattice parameter parallel to the interface between the two multilayer components, is identical for the two components by construction and deviates from Vegard's law. The out-of-plane lattice parameters, defined as the lattice parameters in the directions perpendicular to the interface, are different in the two components which is impossible to obtain for a multilayer where only Vegard's law behavior is

assumed. Furthermore, the c/a ratio, which here is defined as the quotient between the largest and smallest value of the in- and out-of-plane lattice parameters, shows large deviations from unity depending on the relative amount of Fe and $W_{0.8}Re_{0.2}$ components. This model is proposed to yield good structures for multilayers, upon which more accurate calculations can be based.

7. Conclusion and outlook

This thesis has been concerned with the application of theoretical methods to investigate properties related to chemical bonding and structure of materials. In essence two different types of materials have been investigated: transition metal carbides and multilayers. First principles density functional theory calculations have been used extensively to calculate properties of alloyed solutions of transition metal carbides where a stable monocarbide has been alloyed with metal atoms that by themselves possess a weak ability to form carbides. The alloying results in a metastable phase which allow for decomposition into more stable phases. For example, carbon has been shown to be released from the carbides as a response to the alloying. This carbon release was also found to yield lowered friction coefficients which extends the usefulness of the transition metal carbides when regarding industrial applications. To continue the study of these alloyed carbides it would be interesting to study the decomposition of these materials in more detail. Kinetic Monte Carlo simulations would be a perfect tool for such studies since by using this method it is possible to simulate growth processes as well as diffusion processes at any temperature in an efficient manner.

The principle of alloying transition metal carbides to increase the functionality of the carbide phases can also be used for other systems, such as the MAX phases or the transition metal nitrides. In those cases the aim will not be to make them release carbon but other properties could be affected due to the alloying, such as the hardness or the conductivity of the material.

Interface properties of TiC and carbon were investigated between the TiC(111) surface and carbon in the form of graphene/graphite in order to model carbide grain to carbon matrix interactions in nc-TiC/a-C and to investigate the properties of graphene on TiC. The carbon was found to be strongly bonded to the carbide surface. Furthermore, the interface properties were discovered to depend on the termination of the carbide. The theoretical studies on the interface properties performed here are limited when it comes to the size of the system of interest and to simulate grains of carbides in a carbon matrix is impossible using modern implementations of density functional theory calculations. For this reason, it would be interesting to use for example molecular dynamics with classical force fields or a parametrized tight binding method to perform calculations for much larger systems with carbide grains dispersed in a carbon matrix.

For multilayered systems, a model based on elasticity theory has been investigated that in a simple fashion makes it possible to calculate reliable structural parameters. The model can be useful as a starting point for accurate first principles calculations and as an aid in the evaluation of experimental data. What remains to be done is to extend the model to general geometries. So far the model has been set up to be able to calculate the structural parameters for cubic multilayers. Many different geometries can be imagined however, and to extend the model to work for these geometries is a natural step.

8. Svensk sammanfattning

Vi lever i en värld som styrs av partiklar och deras interaktioner. Det finns elektroner, kvarkar, neutriner och alla andra partiklar som tillsammans utgör det stora utbudet av partiklar som beskrivs av standardmodellen. För vår vardag är de viktigaste partiklarna elektronerna. Tillsammans med protoner och neutroner, utgör elektronerna grunden för alla grundämnen i periodiska systemet. Det är elektronerna och deras samspel som avgör hur molekyler bildas av atomer och hur atomer kombineras för att bilda fasta ämnen. Inom materialfysiken är målet att kunna förstå egenskaper hos olika typer av material, från atomnivå till kondenserade former av materia som kristaller och vätskor.

I denna avhandling används teoretiska metoder som grundar sig på första principer för att besvara frågor angående kemisk bindning, struktur och stabilitet hos material som är av stort intresse, både från ett rent vetenskapligt och ur ett industriellt perspektiv. I stor utsträckning handlar denna avhandling om egenskaper hos metallkarbider. I Figur 8.1 finns en illustration av vanligt förekommande kristallstrukturer hos metallkarbider. Dessa material har un-

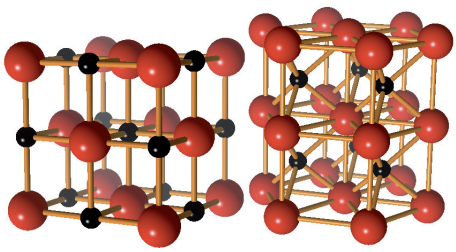

(a) (b)

Figure 8.1: Illustration av kristallstrukturen hos metallkarbider i B1- eller NaCl-strukturen (a) och i B_h- eller WC-strukturen (b). De röda sfärerna representerar metallatomer medans de svarta sfärerna representerar kolatomer.

der lång tid varit av intresse på grund av sina många intressanta fysikaliska egenskaper. På grund av deras kombination av intressanta egenskaper har de blivit använda i många olika tekniska tillämpningar. Ett exempel på en sådan tillämpning är som hårda metallytebeläggningar på olika komponenter. Materials ytor täcks ofta av olika ytbeläggningar för att skydda ytan och där igenom

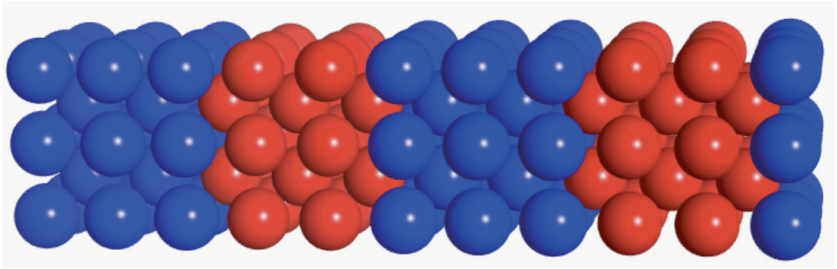

Figure 8.2: Illustration av ett multilagermaterial där olika atomer är markerade med olika färg.

förlängs livstiden för olika komponenter. Därför är det naturligt att mycket energi har lagts på att ta fram nya ytbeläggningsmaterial. Som en del i denna avhandling presenteras en strategi med vilken det är möjligt att framställa nya ytbeläggningar med utökade egenskaper.

En traditionell kristall är ett arrangemang av atomer i någon form av kristallstruktur. Detta är i princip en homogen ordning med identiska positioner i kristallen där atomer populerar de olika positionerna i strukturen. Numera är det praktisk möjligt att skapa nya typer av strukturer där atomerna arrangerats i ett specifikt mönster. Ett sådant material är så kallade multilagermaterial där olika typer av material arrangerats i olika, på varandra följande, lager. I Figur 8.2 finns en illustration av strukturen hos ett multilagermaterial. Det har visat sig att dessa typer av material har nya egenskaper och funktioner, ett exempel är upptäckten av den gigantiska magnetoresistanseffekten (GMR) för vilken Albert Fert och Peter Grünberg belönades med Nobelpriset i fysik 2007.

Teoretiska undersökningar har alltid spelat en avgörande roll för förståelsen av den fysiska världen. Syftet är här att få en beskrivning av alla partiklar och hur de samverkar genom att veta endast antalet partiklar och genom att basera beskrivningen på grundläggande naturlagar, dvs från första principer eller *ab initio*. För en kristall eller en vätska är det mycket komplicerat att teoretiskt modellera och beräkna olika fysiska egenskaper på ett sådant sätt. Detta beror på det stora antalet partiklar som utgör dessa mångpartikelsystem. För att komma vidare är det nödvändigt att utföra en serie approximationer och att konstruera bra modeller. I detta arbete har täthetsfunktionalteorin[1, 2], vilken utvecklades av Walter Kohn och hans medarbetare, använts för att beräkna olika materials egenskaper. Kärnan i täthetsfunktionalteorin är att omvandla problemet med många interagerande partiklar till ett effektivt enpartikelproblem som är mycket lättare att lösa. Olika implementationer av täthetsfunktionalteorin är idag bland de mest använda metoderna för att utföra beräkningar av elektronstrukturen hos olika material.

Denna avhandling är uppdelad i två delar. I del I presenteras vanligt förekommande teorier för kristaller vilka använts flitigt i denna avhandling. Denna del av avhandlingen är inte materialspecifik och diskussionen kan tillämpas på vilket material som helst. Del II är en sammanfattning av de forskningsresultat som presenteras i de medföljande forskningsrapporterna tillsammans med ytterliggare diskussion gällande egenskaper hos metallkarbider och multilagerstrukturer.

9. Acknowledgements

This thesis could not have been completed without the help of several individuals. First of all I want to thank my supervisors Olle Eriksson and Biplab Sanyal for their support and for allowing me to do this work at the Division for Materials Theory. Secondly, I want to thank all of my collaborators for their hard work. Many thanks to Erik, Ola, Stojanka, Mattias L, Urban, Peter and Ulf for giving me an insight into the experimental reality. Thank you Anders, Mattias K, Anna, Petros, Andreas, Lars and Malin for interesting discussions and fruitful collaborations.

Working in the Division for Materials Theory is never dull due to the many individuals that have roamed the corridors during my research studies. Food fascism and the constant flow of bad jokes are everyday elements that will be dearly missed. Thanks to all the members of the group, past and present.

I would like to thank the people with whom I have shared my office: Torbjörn, Duck Young, Ralph, Martin and Peter. Thank you guys for your constant slurping of coffee and continuous talking in the telephone. With roommates like you, no wonder I'm working much better from home. Honestly, however, it has been fun and I appreciate our discussions. It's definitely the best office in the house.

Many thanks goes out to the kind individuals who helped me in proof reading this thesis. Thank you Lars, Anders and Diana for your comments and helpful advices. Also thank you Oscar, Johan and Patrik for always listening when I have some strange ideas and for nice discussions. A special thanks to Love who taught me so many useful things to say in french. Thank you Jonas for the great master thesis project that started my career at the Division for Materials Theory. Furthermore, I want to thank Anders for inviting me into the gang when I first started working on my master thesis. Also, thank you Lars for being my car pooling friend.

A large thanks goes to my family for their support and confidence in me.

Finally, I want to thank the most important person in my life. Ann-Sofie, you're amazing and nothing would be as fun if you were not by my side.

Bibliography

[1] P. Hohenberg and W. Kohn. Inhomogeneous electron gas. *Physical Review B*, 136:B864, 1964.

[2] W. Kohn and L. J. Sham. Self-consistent equations including exchange and correlation effects. *Physical Review*, 140:A1133, 1965.

[3] M. Born and R. Oppenheimer. Zur Quantentheorie der Molekeln. *Annalen der Physik*, 389:457–484, 1927.

[4] N. W. Ashcroft and N. D. Mermin. *Solid State Physics*. Thomson Learning Inc, Philadelphia, 1976.

[5] H. Hellmann. *Einführung in die Quantumchemie*. Franz Deutsche, Leipzig, 1937.

[6] R. Feynman. Forces in molecules. *Physical Review*, 56:340, 1939.

[7] R. Vuilleumier. Density functional theory based *ab initio* molecular dynamics using the Car-Parrinello approach. In M. Ferrario, G. Ciccotti, and K. Binder, editors, *Computer Simulations in Condensed Matter: From Materials to Chemical Biology*, volume 1, pages 223–285. Springer, 2006.

[8] R. Car and M. Parrinello. Unified approach for molecular dynamics and density-functional theory. *Physical Review Letters*, 55:2471, 1985.

[9] D. Frenkel and B. Smit. *Understanding Molecular Simulation: From Algorithms to Applications*. Academic Press, 1996.

[10] M. Payne, M. Teter, D. Allan, T. Arias, and J. D. Joannopoulos. Iterative minimization techniques for ab initio total-energy calculations: molecular dynamics and and conjugate gradients. *Reviews of Modern Physics*, 64:1045–1097, 1992.

[11] S. Baroni, S. de Gironcoli, A. Dal Corso, and P. Giannozzo. Phonons and related crystal properties from density functional perturbation theory. *Reviews of Modern Physics*, 73:515–562, 2001.

[12] D. Alfé. Phon: A program to calculate phonons using the small displacement method. *Computer Physics Communications*, 180:2622–2633, 2009.

[13] P. Souvatzis, O. Eriksson, M. I. Katsnelson, and S. P. Rudin. The self-consistent *ab initio* lattice dynamical method. *Computational Materials Science*, 44:888–894, 2009.

[14] D. Pettifor. *Bonding and structure of molecules and solids*. Oxford University Press, Oxford, 1995.

[15] F. Ducastelle. *Order and phase stability in alloys*. North Holland, Amsterdam, 1991.

[16] A. V. Ruban and I. A. Abrikosov. Configurational thermodynamics of alloys from first principles: effective cluster interactions. *Reports on Progress in Physics*, 71:046501, 2008.

[17] P. A. Korzhavyi, A. V. Ruban, I. A. Abrikosov, and H. L. Skriver. Madelung energy for random metallic alloys in the coherent potential approximation. *Physical Review B*, 51:5773, 1995.

[18] A. Zunger, S.-H. Wei, L. G. Ferreira, and J. E. Bernard. Special quasirandom structures. *Physical Review Letters*, 65:353–356, 1990.

[19] S.-H. Wei, L. G. Ferreira, J. E. Bernard, and A. Zunger. Electronic properties of random alloys: Special quasirandom structures. *Physical Review B*, 42:9622–9649, 1990.

[20] R. G. Parr and W. Yang. *Density Functional Theory of Atoms and Molecules*. Oxford University Press, New York, 1989.

[21] R. M. Martin. *Electronic Structure, Basic Theory and Practical Methods*. Cambridge University Press, Cambridge, 2004.

[22] R. M. Dreizler and E. K. U. Gross. *Density Functional Theory*. Springer, Berlin, 1990.

[23] R. O. Jones and O. Gunnarsson. The density functional formalism, its applications and prospects. *Reviews of Modern Physics*, 61:689–746, 1989.

[24] S. Kurth, J. P. Perdew, and P. Blaha. Molecular and Solid-State Tests of Density Functional Approximations: LSD, GGAs, and Meta-GGAs. *International Journal of Quantum Chemistry*, 75:889–909, 1999.

[25] U. von Barth and L. Hedin. A local exchange-correlation potential for the spin polarized case. 1. *Journal of Physics C: Solid State Physics*, 5:1629–1642, 1972.

[26] S. H. Vosko, L. Wilk, and M. Nusair. Accurate spin-dependent electron liquid correlation energies for local spin-density calculations - a critical analysis. *Canadian Journal of Physics*, 58:1200–1211, 1980.

[27] A. Becke. Density-functional exchange-energy approximation with correct asymptotic behavior. *Physical Review A*, 38:3098, 1988.

[28] J. P. Perdew and Y. Wang. Accurate and simple analytic representation of the electron-gas correlation energy. *Physical Review B*, 45:13244–13249, 1992.

[29] J. Perdew, K. Burke, and M. Ernzerhof. Generalized gradient approximation made simple. *Physical Review Letters*, 77:3865, 1996.

[30] P. E. Blöchl. Generalized separable potentials for electronic-structure calculations. *Physical Review B*, 41:5414–5416, 1990.

[31] D. Vanderbilt. Soft self-consistent pseudopotentials in a generalized eigenvalue formalism. *Physical Review B*, 41:7892, 1990.

[32] P. E. Blöchl. Projector augmented-wave method. *Physical Review B*, 50:17953–17979, 1994.

[33] G. Kresse and D. Joubert. From ultrasoft pseudopotentials to the projector augmented-wave method. *Physical Review B*, 59:1758, 1999.

[34] L. E. Toth. *Transition Metal Carbides and Nitrides*. Academic Press, New York, 1971.

[35] K. Schwarz. Band structure and chemical bonding in transition metal carbides and nitrides. *CRC Critical Reviews in Solid State and Materials Sciences*, 13:211–257, 1987.

[36] H. W. Hugosson. *A Theoretical Treatise on the Electronic Structure of Designer Hard Materials*. PhD thesis, Uppsala University, 2001.

[37] W. S. Williams. Cubic carbides. *Science*, 152:34–42, 1966.

[38] P. Ettmayer and W. Lengauer. Carbides: Transition metal solid state chemistry. In R. B. King, editor, *Encyclopedia of Inorganic Chemistry*. John Wiley & Sons Ltd., 1994.

[39] S. V. Meschel and O. J. Kleppa. Standard enthalpies of formation of some 3d transition metal carbides by high temperature reaction calorimetry. *Journal of Alloys and Compounds*, 257:227, 1997.

[40] E. Lewin. *Design of carbide-based nanocomposite coatings*. PhD thesis, Uppsala University, 2009.

[41] C. D. Gelatt, A. R. Williams, and V. L. Moruzzi. Theory of bonding of transition metals to nontransition metals. *Physical Review B*, 27:2005, 1983.

[42] J. Häglund, G. Grimvall, T. Jarlborg, and A. Fernández Guillermet. Band structure and cohesive properties of 3d-transition-metal carbides and nitrides with the NaCl-type structure. *Physical Review B*, 43:14400, 1991.

[43] A. Fernández Guillermet, J. Häglund, and G. Grimvall. Cohesive properties of 4d-transition-metal carbides and nitrides in the NaCl structure. *Physical Review B*, 45:11557, 1992.

[44] A. Fernández Guillermet, J. Häglund, and G. Grimvall. Cohesive properties of 5d-transition-metal carbides and nitrides in the NaCl structure. *Physical Review B*, 48:11673, 1993.

[45] J. Häglund, A. Fernández Guillermet, and G. Grimvall. Theory of bonding in transition-metal carbides and nitrides. *Physical Review B*, 48:11685, 1993.

[46] A. Grechnev, R. Ahuja, and O. Eriksson. Balanced crystal orbital overlap population - a tool for analyzing chemical bonds in solids. *Journal of Physics: Condensed Matter*, 15:7751, 2003.

[47] E. I. Isaev, R. Ahuja, S. I. Simak, A. I. Lichtenstein, Y. K. Vekilov, B. Johansson, and I. A. Abrikosov. Anomalously enhanced superconductivity and *ab initio* lattice dynamics in transition metal carbides and nitrides. *Physical Review B*, 72:064515, 2005.

[48] E. I. Isaev, S. I. Simak, I. A. Abrikosov, R. Ahuja, Y. K. Vekilov, M. I. Katsnelson, A. I. Lichtenstein, and B. Johansson. Phonon related properties of transition metals, their carbide, and nitrides: A first principles study. *Journal of Applied Physics*, 101:123519, 2007.

[49] H. Jónsson, G. Mills., and K. W. Jacobsen. Nudged elastic band method for finding minimum energy paths of transitions. In B. J. Berne, G. Ciccotti, and D. F. Coker, editors, *Classical and Quantum Dynamics in Condensed Phase Simulations*, page 385. World Scientific, 1998.

[50] G. Henkelman, B. P. Uberuaga, and H. Jónsson. A climbing image nudged elastic band method for finding saddle points and minimum energy paths. *Journal of Chemical Physics*, 113:9901, 2000.

[51] G. Henkelman and H. Jónsson. Improved tangent estimate in the nudged elastic band method for finding minimum energy paths and saddle points. *Journal of Chemical Physics*, 113:9978, 2000.

[52] D. Sheppard, R. Terrel, and G. Henkelman. Optimization methods for finding minimum energy paths. *Journal of Chemical Physics*, 128:134106, 2008.

[53] A. K. Geim and K. S. Novoselov. The rise of graphene. *Nature Materials*, 6:183, 2007.

[54] M. I. Katsnelson. Graphene: carbon in two dimensions. *Materials Today*, 10:20, 2007.

[55] R. Bader. *Atoms in Molecules: A Quantum Theory*. Oxford University Press, New York, 1990.

[56] G. Henkelman, A. Arnaldsson, and H. Jónsson. A fast and robust algorithm for bader decomposition of charge density. *Computational Materials Science*, 36:254–360, 2006.

[57] E. Sanville, S. D. Kenny, R. Smith, and G. Henkelman. An improved grid-based algorithm for bader charge allocation. *Journal of Computational Chemistry*, 28:899–908, 2007.

[58] W. Tang, E. Sanville, and G. Henkelman. A grid-based bader analysis algorithm without lattice bias. *Journal of Physics: Condensed Matter*, 21:084204, 2008.

[59] W. Kohn and N. Rostoker. Solution of the schrödinger equation in periodic lattices with an application to metallic lithium. *Physical Review*, 94:111–1120, 1954.

[60] J. Korringa. On the calculation of the energy of a bloch wave in a metal. *Physica*, 13:392–400, 1947.

[61] I. A. Abrikosov and H. L. Skriver. Self-consistent linear-muffin-tin-orbitals coherent-potential technique for bulk and surface calculations: Cu-Ni, Ag-Pd, and Au-Pt random alloys. *Physical Review B*, 81:014405, 1993.

[62] A. V. Ruban and H. L. Skriver. Calculated surface segregation in transition metal alloys. *Computational Materials Science*, 15:119–143, 1999.

Acta Universitatis Upsaliensis

Digital Comprehensive Summaries of Uppsala Dissertations from the Faculty of Science and Technology 749

Editor: The Dean of the Faculty of Science and Technology

A doctoral dissertation from the Faculty of Science and Technology, Uppsala University, is usually a summary of a number of papers. A few copies of the complete dissertation are kept at major Swedish research libraries, while the summary alone is distributed internationally through the series Digital Comprehensive Summaries of Uppsala Dissertations from the Faculty of Science and Technology. (Prior to January, 2005, the series was published under the title "Comprehensive Summaries of Uppsala Dissertations from the Faculty of Science and Technology".)

Distribution: publications.uu.se
urn:nbn:se:uu:diva-123485

ACTA
UNIVERSITATIS
UPSALIENSIS
UPPSALA
2010